Electronic supplementary materials *Mendeleev Commun.*, 2020, **30**, 456–458

CoO-$x$$Co(OH)_2$ supported silver nanoparticles: electrosynthesis in acetonitrile and catalytic activity

Rezeda R. Fazleeva, Gulnaz R. Nasretdinova, Yury N. Osin, Aida I. Samigullina, Aidar T. Gubaidullin and Vitaliy V. Yanilkin

Experimental

Preparative electrolysis was carried out in a three-electrode diaphragm-separated (porous glass) and undivided glass cells in potentiostatic mode at room temperature (T = 295 K) using a P-30S potentiostat. The solution was stirred with a magnetic stirrer during electrolysis. A glassy carbon (GC) plate (S = 3.2 cm^2) was used as the working electrode; an aqueous saturated calomel electrode (SCE) was used as the reference electrode. The latter was connected with the solution being studied through a bridge containing the supporting electrolyte. A platinum wire was used as the auxiliary electrode in the electrolyses in a divided cell, and a cobalt plate was used as the auxiliary electrode in an undivided cell. Acetonitrile (AN) was the solvent, and 0.1 M Bu_4NBF_4 was chosen as the supporting electrolyte. In the electrolysis in an undivided cell, Co^{2+} ions were supplied into solution during electrolysis by dissolution of the anode metal and the obtained particles of support were designated CoO-x$Co(OH)_2$ in the absence of PVP and CoO-x$Co(OH)_2$/PVP in the presence. In the electrolysis in a divided cell, the AN/0.1 M Bu_4NBF_4 solution was placed in the auxiliary anodic compartment; Ag^+ ions were added to the CoO-x$Co(OH)_2$ solution as a salt and the obtained nanocomposites were designated Ag/CoO-x$Co(OH)_2$ and Ag/CoO-x$Co(OH)_2$/PVP depending on absence or presence of stabilizer.

CoO-x$Co(OH)_2$ and CoO-x$Co(OH)_2$/PVP preparation. A working solution (24 ml) for the electrolysis contains only supporting electrolyte (experiment 1), supporting electrolyte and stabilizer poly(N-vinylpyrrolidone) (PVP) (experiment 2). The Co-anode area was 5.32 cm^2.

Ag/CoO-x$Co(OH)_2$ and Ag/CoO-x$Co(OH)_2$/PVP preparation. 4.1 mg $AgNO_3$ (1.5mM) was added to the 16 ml of CoO-x$Co(OH)_2$ solutions, obtained in experiments 1 and 2. Half of the solution (8 ml) was isolated for study (experiments 1-1, 2-1), the other half was subsequently electroreduced (experiments 1-2, 2-2).

The resulting solutions obtained after electrolysis were studied by cyclic voltammetry (CV), scanning (SEM) and transmission (TEM) electron microscopy, X-ray powder diffraction (XRPD), UV-visible (UV-VIS) and infrared (IR) spectroscopy, dynamic light scattering (DLS) and was tested for catalytic activity.

For the study by SEM, TEM, XRPD, as well as UV-VIS and DLS, the NP obtained in the experiments 1, 1-2, 2 and 2-2 were precipitated by centrifugation (14 500 rpm, 3 hours), were washed with AN and twice with ethanol. The washing consisted in dispersing the precipitate in the solvent by sonication and subsequent precipitation by centrifugation (14 500 rpm, one hour (exp. 1 and 1-2) and 3 hours (exp. 2 and 2-2)).

For SEM, the resulting solution was applied onto a titanium foil surface preliminarily cleaned by ultrasonic treatment in water, acetone, and ethanol. After that, the sample was dried at room temperature. In the case of TEM, 5 μl of the solution was placed on a 3 mm copper mesh with formvar/carbon (Formvar/Carbon, Lacey Formvar) support and dried at room temperature. After complete drying, the mesh in a special graphite holder was placed into a transmission electron microscope in order to perform the microanalysis.

CV. Cyclic voltammograms (CV curves) were recorded using the P-30S potentiostat (without IR compensation). A GC disc electrode (dia. 2.0 mm) sealed into a glass tube was used as the working electrode. Prior to each measurement, the electrode was mechanically polished. A platinum wire was used as the auxiliary electrode. Potentials were measured *versus* SCE connected to the solution being studied through a bridge containing the supporting electrolyte and having a potential of -0.41 V relative to formal potential E_0' $Fc^{+/0}$ (internal standard). The temperature was 295 K.

UV-VIS. Absorption spectra were recorded on a Perkin-Elmer Lambda 25 spectrometer.

IR. IR spectra were recorded for KBr pellets in the range of 4000–400 cm^{-1} on a Bruker Tensor 27 spectrometer with optical resolution of 4 cm^{-1} and accumulation of 64 scans.

DLS. The measurements were performed using a Malvern Instrument Zetasizer Nano. The measured autocorrelation functions were analyzed with Malvern DTS software.

Electron microscopic analysis. The SEM studies were carried out using a Merlin field emission scanning electron microscope (Carl Zeiss, Germany). The surface morphology was imaged in the secondary electron (SE) mode with the primary electron accelerating voltage of 5 kV and with the probe current of 300 pA, to minimize the exposure to the object of study. To detect phase contrast, the accelerating voltage of primary electrons was 20 kV, and the probe current was 1 nA. The survey was carried out in the back-scattered electrons (AsB) mode. The

microscope was equipped with an AZtec X-MAX energy dispersion spectrometer (Oxford Instruments, Great Britain) with a resolution of 127 eV. The precision of measurement was 0.01-1%. The elemental analysis was carried out at the accelerating voltage of 20 keV and the flange focal length of 9.6 mm, which allowed minimizing the errors. The probing depth was less than 1 μm. In the quantitative analysis, a set of etalons incorporated to the Aztec program (reference standard for X-RAY microanalysis "Registered Standart No. 8842") was used.

TEM-studies were carried out in the HR-TEM mode using a Hitachi HT 7700 Exalens (Japan) transmission electron microscope at the accelerating voltage of 100 keV with a resolution of 0.144 nm. The elemental analysis was carried out using an Oxford Instruments X-Max^n 80T (Great Britain) attachment equipped with a special holder.

XRPD. The measurements were performed on a Bruker D8 Advance diffractometer equipped with Vario attachment and Vantec linear PSD, using Cu radiation (40 kV, 40 mA) monochromated by the curved Johansson monochromator (λ Cu $K_{\alpha 1}$ 1.5406 Å). Room-temperature data were collected in the reflection mode with a flat-plate sample.

The samples in liquid form were loaded on a silicon plate, which reduces background scattering. To increase the total amount of the sample, several more layers were applied on top of the first one after it dried. Patterns were recorded in the 2Θ range between 3^o and 90^o, in 0.008^o steps, with a step time of 0.1–4.0s. Several diffraction patterns in various experimental modes and with different data accumulation time were collected and summed. The dried samples were scraped off the surface of the plate and, in the form of a powder, were replaced on a silicon plate to perform the verification experiment for the presence of preferential orientation of crystallites. To correct the angular position of peaks, additional experiments were performed with each sample with the addition of SRM676 corundum powder as an internal standard.

Processing of the obtained data was performed using EVA [1] and TOPAS [2] software packages. The crystallite size calculations were performed using the TOPAS software package in several ways: the values calculated from the half-width of the reflections (LVol-FWHM) and the integrated reflection intensity (LVol-IB) are the volume-weighted values of the crystallite sizes, and the CrySizeL parameter is the size of the crystallites in the direction perpendicular to the analyzed planes, with the Lorentz type of peak broadening. The minimization of the discrepancy between the experimental and calculated data in the refinement process was performed by the Rietveld method over the entire array of experimental data. Minimization in the process of the R_{wp} and R_{exp} convergence parameters verifying was used as a criterion of correct comparison of

the calculated and experimental data. ICDD PDF-2 Release 2005 powder diffraction database was used for the identification of crystalline modifications.

Catalytic reduction of p-nitrophenol with sodium borohydride in the presence of CoO-xCo(OH)$_2$, CoO-xCo(OH)$_2$/PVP supports and Ag/CoO-xCo(OH)$_2$, Ag/CoO-xCo(OH)$_2$/PVP nanocomposites. In a quartz cuvette (l = 0.5 cm), 2 μl of the CoO-xCo(OH)$_2$, CoO-xCo(OH)$_2$/PVP supports and Ag/CoO-xCo(OH)$_2$, Ag/CoO-xCo(OH)$_2$/PVP nanocomposites solutions, obtained in the electrolyses in AN, were added to 1.5 ml of an aqueous solution containing 0.1 mM *p*-nitrophenol and 5 mM $NaBH_4$. The reaction was controlled by changes in the optical density of *p*-nitrophenol at 400 nm over time at 295 K.

Reagents. Commercially available $AgNO_3$, Bu_4NBF_4 («Aldrich»), PVP (40 000 D) («Alfa Aesar») and AN («Acros Organics») were used without additional purification. In all media used all salts dissociate fairly well. Therefore, we operate mainly with ions. The investigated solutions contained water which amount is the sum of: (i) the residual amount of water in DMF; (ii) the water introduced with any of the reactants; (iii) the increasing amount of water absorbed from the air over time since the solutions are in constant contact with the air.

References

1. *EVA v.11.0.0.3, User Manual*, SOCABIM, 2005.

2. *TOPAS V3, General profile and structure analysis software for powder diffraction data, Technical Reference*, Bruker AXS, Karlsruhe, Germany, 2005.

Table S1. The potentials (V *vs.* SCE) of reduction (E_C) and reoxidation (E_A) peaks of investigated substrates on the GC electrode in AN/0.1 M Bu_4NBF_4

Substrate	E_{C1}^{Co}	E_{C2}^{Co}	E_A^{Co}	E_{C1}^{O2}	E_{C1}^{Ag}	E_{C2}^{Ag}	E_{A1}^{Ag}	E_{A2}^{Ag}
Co^{2+}	-0.93	-1.28	+0.27					
O_2				-0.99				
Ag^+					0.02		0.39	
O_2+Co^{2+}	-1.05			-1.05				
CoO-xCo(OH)$_2$								
O_2 + CoO-xCo(OH)$_2$				-0.99				
O_2+ CoO-xCo(OH)$_2$ +Ag^+				-1.02	0.02		0.40	

O_2+ CoO-x$Co(OH)_2$ +Ag^0				-0.96				
CoO-x$Co(OH)_2$ +PVP								
O_2 + CoO-x$Co(OH)_2$ +PVP				-0.98				
O_2+ CoO-x$Co(OH)_2$ +Ag^++PVP				-0.99	0.04	-0.54	0.34	-0.16
O_2+ CoO-x$Co(OH)_2$ +Ag^0+PVP				-0.98				

Table S2. Lattice parameters, crystallite average sizes of Ag in Ag/CoO-x$Co(OH)_2$ (experiment 1-2) and Ag/CoO-x$Co(OH)_2$/PVP (experiment 2-2) nanocomposites

Experiment No	1-2				2-2
Miller Indices	111	200	220	311	111
Angle 2θ, º	38.137(1)	44.318(8)	64.472(7)	77.405(8)	38.296(9)
CrySizeL (nm)	51.7(11)	17.48(90)	48.5(48)	49.3(55)	4.6(1)
LVol-IB (nm)	32.89(71)	11.13(17)	30.9(30)	31.4(35)	2.90(7)
Lvol-FWHM (nm)	45.98(99)	15.56(80)	43.1(42)	43.9(49)	4.06(9)
R_{exp}	5.66%				1.64%
R_{wp}	2.17%				1.95%

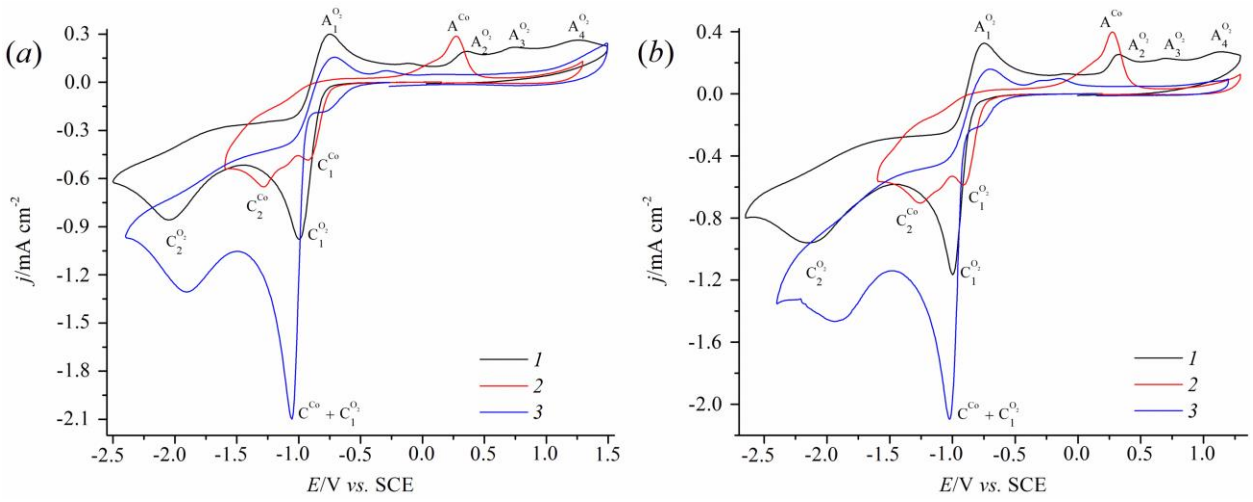

Figure S1. CV curves of dissolved O_2 (~3.3 mM) (*1*), Co^{2+} (3 mM) (*2*) and the (O_2 + 3 мМ Co^{2+}) system (*3*) in the absence (*a*) and in the presence (*b*) of 20 mM PVP, GC, AN/0.1 M Bu_4NBF_4, ν = 100 mV/s.

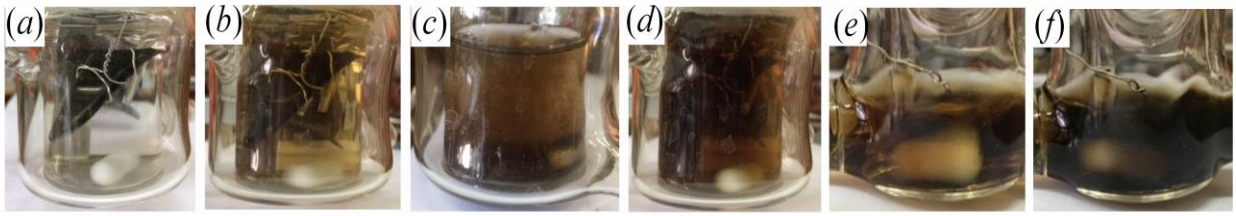

Figure S2. Photos of the (~3.3 mM O_2 + 3 mM Co^{2+}(dissolution of Co-anode)) system in electrolysis cell during the electrolysis at *E* = -1.10 V in AN/0.1 M Bu_4NBF_4 medium after passing various amounts of electricity (F with respect to Co^{2+}): 0 (*a*), 0.2 (*b*), 2.0 (*c*) (experiment 1), 2.0 (experiment 2); and after addition of 1.5 mM $AgNO_3$ to the solution, obtained in experiment 2 (*e*) (experiment 2-1) and subsequent preparative electrolysis at *E* = -1.10 V (*Q* = 1 F with respect to 1.5 mM Ag^+) (*f*) (experiment 2-2).

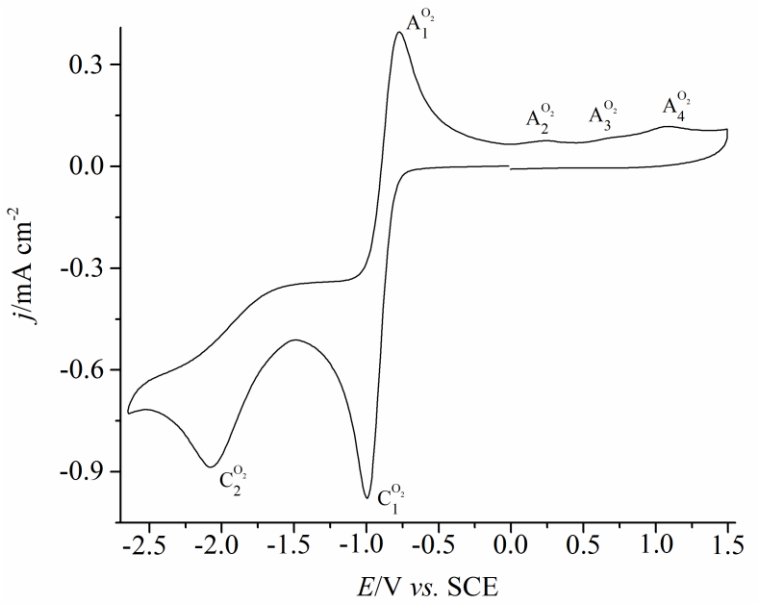

Figure S3. CV curves after the preparative electrolysis of CoO-xCo(OH)$_2$ at E = -1.10 V (Q = 2F with respect to 3mM Co^{2+}) (experiment 1), GC, AN/0.1 M Bu_4NBF_4, ν = 100 mV/s.

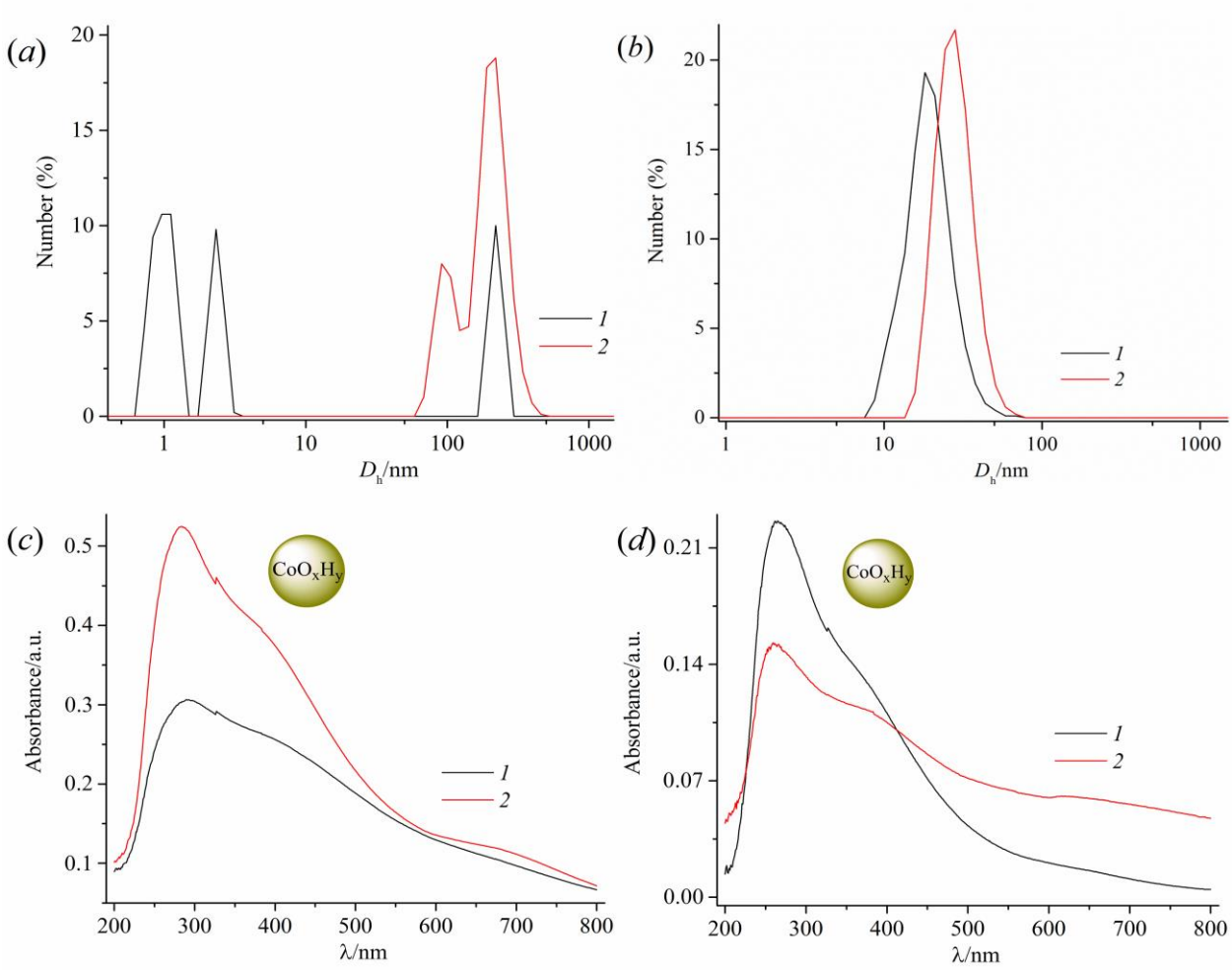

Figure S4. Particle size distribution diagram (DLS) (*a*, *b*) and UV-VIS spectra (*c*, *d*) of CoO-xCo(OH)$_2$ and CoO-xCo(OH)$_2$/PVP supports, obtained by electrolyses 1 (*a*, *c*) and 2 (*b*, *d*): in the solutions after electrolysis (*1*) and in ethanol solutions after dispersion of isolated NPs (*2*).

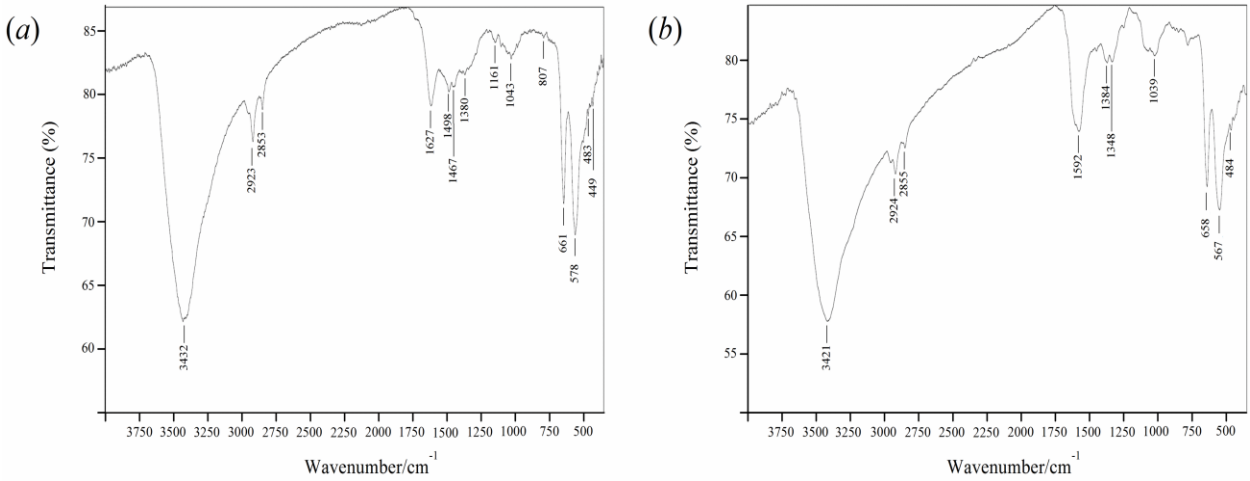

Figure S5. IR spectra of isolated and dried precipitates of CoO-xCo(OH)$_2$ (experiment 1) (*a*) and CoO-xCo(OH)$_2$/PVP (experiment 2) (*b*) supports.

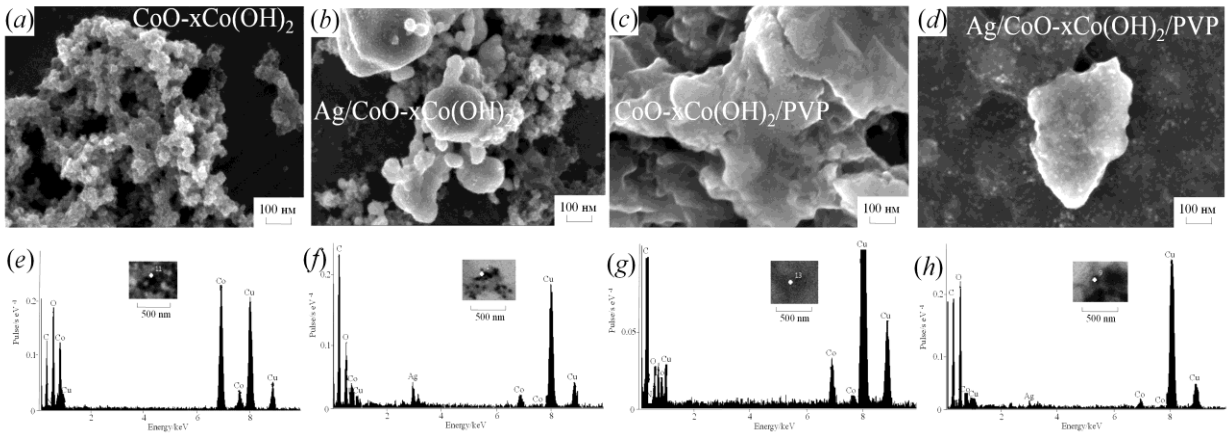

Figure S6. SEM- (*a-d*) and energy dispersive spectra (*e-h*) of CoO-xCo(OH)$_2$, CoO-xCo(OH)$_2$/PVP supports and Ag/CoO-xCo(OH)$_2$, Ag/CoO-xCo(OH)$_2$/PVP nanocomposites, obtained in the electrolyses 1 (*a*, *e*), 1-2 (*b*, *f*), 2 (*c*, *g*) and 2-2 (*d*, *h*). (Cu is from the supports).

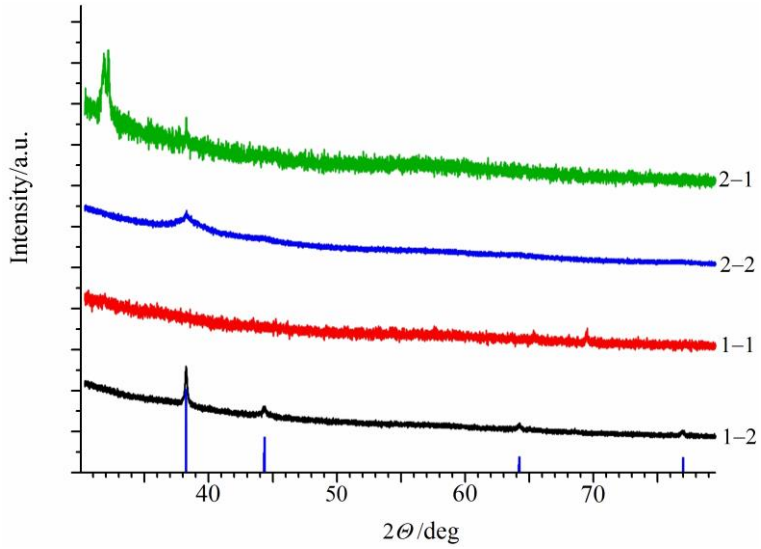

Figure S7. Experimental XRPD patterns of the samples from experiments 1-1, 1-2, 2-1 и 2-2. Interference peaks corresponding to the crystalline form of Ag (Silver, syn., code # 01-087-0720) according to PDF-2 database are shown by vertical dashes.

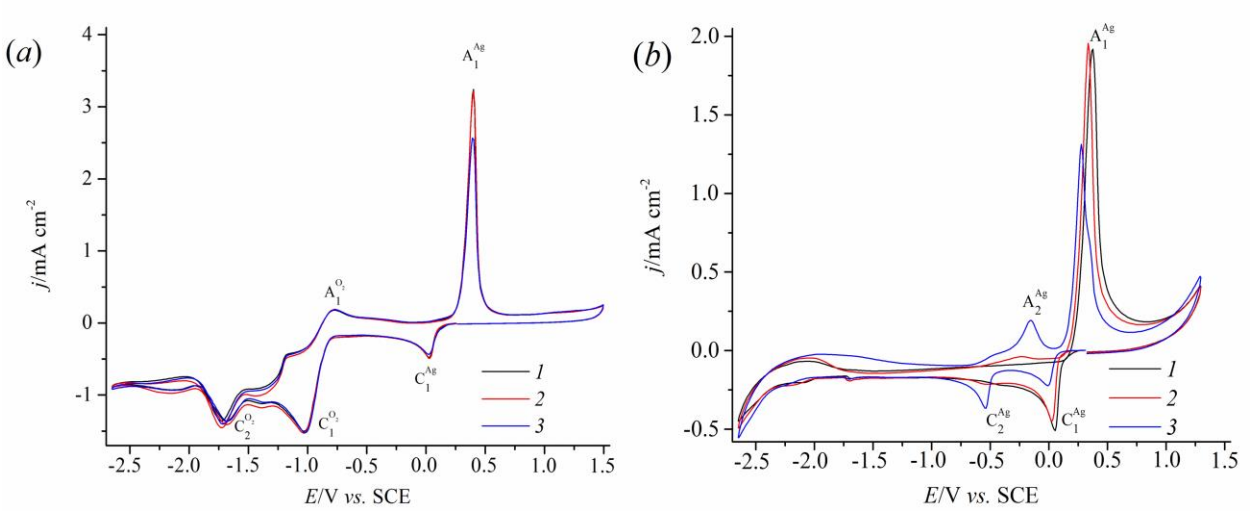

Figure S8. CV curves of (*a*) CoO-xCo(OH)$_2$ + ~3.3 mM O_2 + 1.5 mM $AgNO_3$ (experiment 1-1) и (*b*) CoO-xCo(OH)$_2$/PVP + 1.5 mM $AgNO_3$ (experiment 2-1) systems during time: 10 (*1*), 30 (*2*) and 60 (*3*) min, GC, AN/0.1 M Bu_4NBF_4, ν = 100 mV/s.

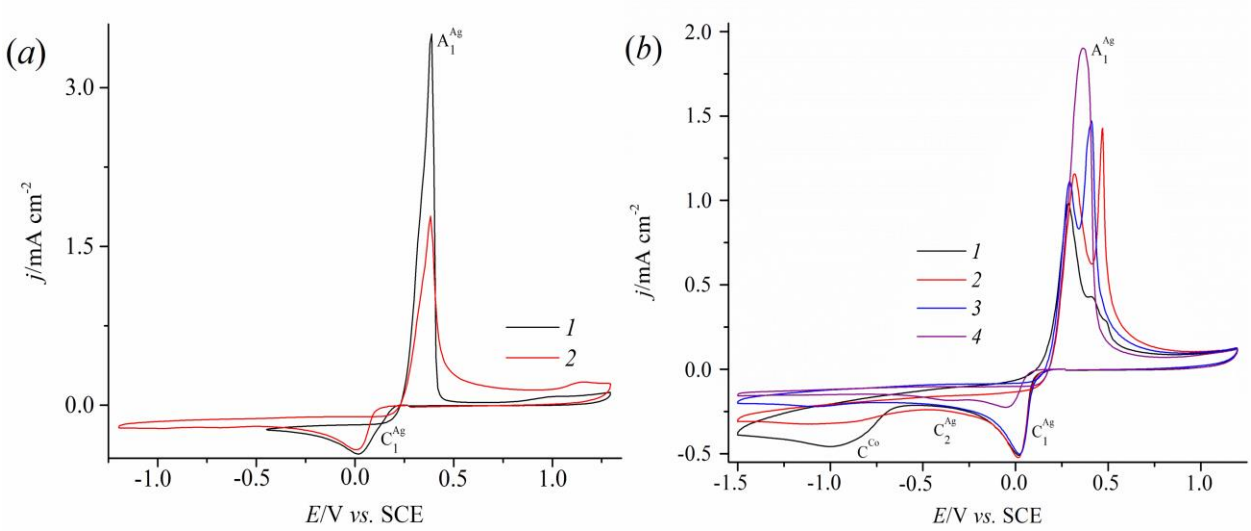

Figure S9. CV curves of (*a*) 1.5 mM $AgNO_3$ in the absence (*1*) and in the presence (*2*) of 20 mM PVP; (*b*) 3 mM $Co(BF_4)_2$ + 1.5 mM $AgNO_3$ + 20 mM PVP (*1*) after addition of certain concentration of Bu_4NOH: 0.40 (*2*), 0.72 (*3*) and 1.5 mM (*4*), GC, AN/0.1 M Bu_4NBF_4, ν = 100 mV/s.

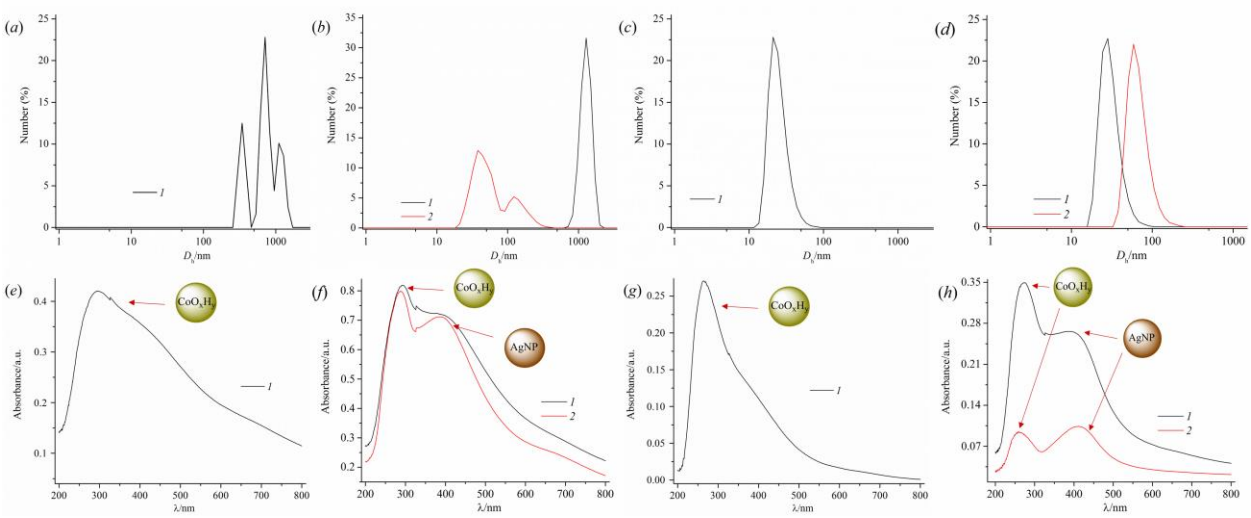

Figure S10. Particle size distribution diagram (DLS) (*a*-*d*) and UV-VIS spectra (*e*-*h*) of CoO-xCo(OH)$_2$ and CoO-xCo(OH)$_2$/PVP supports and Ag/CoO-xCo(OH)$_2$, Ag/CoO-xCo(OH)$_2$/PVP nanocomposites, obtained by electrolyses 1-1(*a*, *e*), 1-2(*b*, *f*), 2-1(*c*, *g*) and 2-2(*d*, *h*): in the solutions after electrolysis (*1*) and in ethanol solutions after dispersion of isolated NPs (*2*).

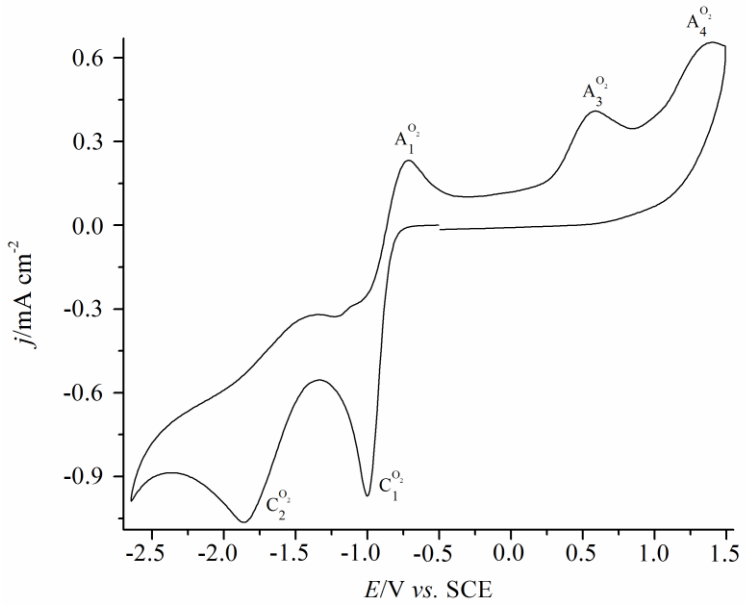

Figure S11. CV curves after the preparative electrolysis of Ag/CoO-xCo(OH)$_2$ (experiment 1-2) at E = -1.10 V (Q = 1F with respect to 1.5 mM Ag^+), GC, AN/0.1 M Bu_4NBF_4, ν = 100 mV/s.

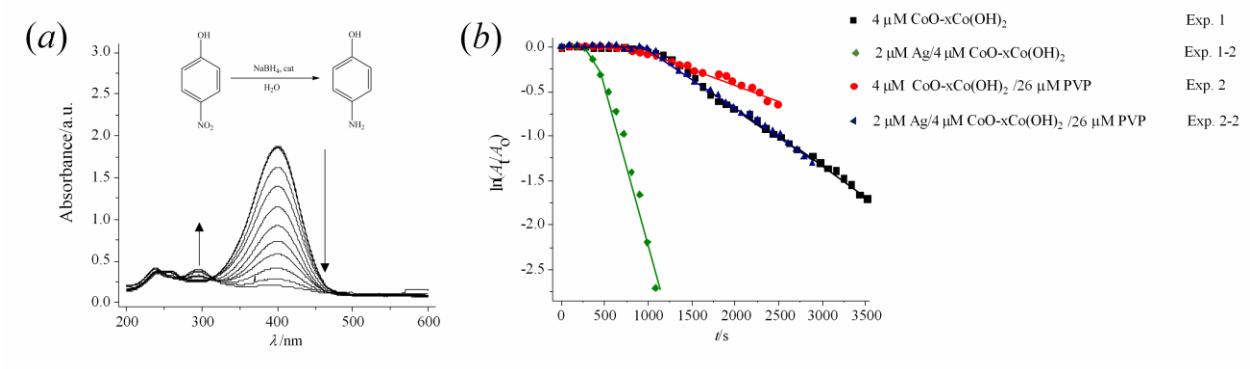

Figure S12. Reduction of *p*-nitrophenol (0.1 mM) with sodium borohydride (5 mM) catalyzed by CoO-xCo(OH)$_2$, CoO-xCo(OH)$_2$/PVP, Ag/CoO-xCo(OH)$_2$ and Ag/CoO-xCo(OH)$_2$/PVP: (*a*) changes in the UV-VIS spectrum of the reaction mixture obtained after addition of catalyst; (*b*) semi-logarithmic kinetic curve, where A_0 is the optical density before addition of catalyst, A_t is the current optical density; H_2O, 25 ^{0}C.